

BEAM CHARACTERIZATION IN THE CEBAF-ER EXPERIMENT*

C. Tennant[#], Y. Chao, D. Douglas, A. Freyberger, M. Tiefenback
 Thomas Jefferson National Accelerator Facility, Newport News, VA 23606, USA

Abstract

Energy recovering a 1 GeV beam through CEBAF (Continuous Electron Beam Accelerator Facility) presents many operational challenges. As a result, it is important to have a quantitative understanding of the beam behavior throughout the machine. The emittance provides a figure of merit in this context inasmuch as it characterizes the extent to which beam quality is preserved during energy recovery. A solution to the problem of obtaining a high-resolution emittance measurement in the extraction region of the CEBAF-ER experiment (CEBAF with Energy Recovery) is presented. The method makes use of a single scanning quadrupole and a downstream wire scanner. In addition, by using multiple wire scans, a scheme for measuring the emittance and momentum spread of the first pass beam in the injector and Arcs 1 and 2 was implemented. And by using a novel technique employing wire scans in conjunction with PMTs (Photomultiplier Tubes) to accurately measure the beam profile at the dump, we can quantify the extent to which we have successfully transported beam to the energy recovery dump.

INTRODUCTION AND MOTIVATION

With several proposals world-wide for machines based on Energy Recovery Linacs (ERLs), there are still important accelerator physics and technological issues that must be resolved before any of these applications can be realized. The Jefferson Lab FEL (Free Electron Laser) upgrade, presently under construction and designed to accelerate 10 mA up to 210 MeV and then subject it to energy recovery will be an ideal test bed for the understanding of high current phenomena in ERL devices. In an effort to address the issues of energy recovering high energy beams, Jefferson Lab has successfully completed a minimally invasive energy-recovery experiment utilizing the CEBAF accelerator [2]. The experiment's goal was to demonstrate the energy recovery of a 1 GeV beam while characterizing the beam phase space at various points in the machine and to measure the RF system's response to energy recovery. Once satisfactory measurements were obtained using the nominal 55 MeV injection energy, the measurements were repeated for low injection energy (20 MeV) to study the parametric dependence on low injection energy to final energy ratios.

PHASE SPACE MEASUREMENTS

To gain a quantitative understanding of the beam behavior through the machine, an intense effort was made to characterize the 6D phase space during the CEBAF-ER experimental run. A scheme has been implemented to measure the geometric emittance of the energy recovered beam prior to being sent to the dump, as well as in the injector and in each arc. In this way we can understand how the emittance evolves through the machine. In addition to describing the transverse phase space, the momentum spread was measured in the injector and arcs to characterize the longitudinal phase space.

Emittance and Momentum Spread in the Injector and Arcs

The emittance and momentum spread of the first pass beam were measured in the injector, Arc 1, and Arc 2 utilizing a scheme involving multiple optics and multiple wire scanners. Two wire scanners were placed in each arc, one at the beginning of the arc in a non-dispersive region and the second in the middle of the arc at a point of high dispersion (6 m). The emittance in the injector was measured using five wire scanners along the injector line.

One of the unresolved difficulties with this measurement was finding a scheme for which the emittance and momentum spread of the *recirculated* beam could be measured in Arc 1. During the measurement an insertable, downstream dump was used to prohibit the transport of a recirculated beam. But it is unclear how to resolve each beam from a wire scanner that is sampling two co-propagating beams; even more so in the case of Arc 1 where, notionally, both the first pass and second pass energy recovered beam have the same energy. This is not an issue for Arc 2; since the energy recovered beam is sent to the dump immediately upon exiting the South Linac, there is at all times only one beam being transported through Arc 2.

Emittance in the Extraction Region

Of great interest is the beam emittance of the energy recovered beam prior to delivery to the dump. Whereas the previous section described the use of multiple wire scanners and multiple optics to obtain the emittances in the injector and Arcs, the emittance in the extraction region relied on a single scanning quadrupole and a wire scanner. The quadrupole at region 2L21 (just after the exit of the South Linac) was scanned and used to obtain the emittance in the horizontal plane while the adjacent, downstream quad at 2L22 was scanned to obtain the vertical emittance. Because of the presence of the two co-propagating beams in the extraction region (the first pass beam at 1055 MeV and the second pass, energy recovered

*supported by US DOE Contract No. DE-AC05-84ER40150

[#]tennant@jlab.org

beam at 55 MeV), care was taken to produce compensatory optics using a family of downstream quads to ensure the first pass beam would be unaffected and transported unaffected through the machine.

By the end of the CEBAF-ER run, data were collected to calculate the emittance in each transverse plane for injection energies of 55 and 20 MeV. All the analysis was done off-line. First, the signals of the raw wire scans were fit with a Gaussian distribution and the sigmas of each extracted. For the case of a quadrupole-drift-wire scanner configuration, one can show that the beam size squared depends quadratically on the quadrupole strength,

$$\sigma_{measured}^2 = \beta_{wire} \epsilon = (1 + kL)^2 (\beta_{quad} \epsilon) - 2L(1 + kL)(\alpha_{quad} \epsilon) + L^2 (\gamma_{quad} \epsilon)$$

where L is the distance from the quadrupole to the wire scanner and k is the quadrupole strength in the thin lens approximation. By plotting the sigmas squared versus the quadrupole strength and performing a least-squares fit, the emittance as well as the Twiss functions at the entrance of the scanning quadrupole can be extracted [3].

There were several challenges in analyzing the data. The first obstacle, as mentioned above, was that all the analysis had to be done off-line. Whereas in normal operation of CEBAF the wire scanner software calculates the sigmas of the signals immediately, due to the fact that the wire was now picking up six distinct signals (a three-wire scanner in the presence of two beams), the software simply fit the first three it encountered. Consequently, it was not immediately known if we had scanned far enough away from the nominal gradient integral to pass through a minimum in spot size. In fact, in two out of our four emittance measurements, we were fitting one-half of a parabola because the quadrupole had not been scanned sufficiently far. A second difficulty we encountered was a fit of the data that resulted in an unphysical (i.e. complex) solution for the emittance. This occurred when the fitting parameters led to the condition that the determinant of the sigma matrix was less than zero, $\epsilon^2 = (\sigma_{11}\sigma_{22} - \sigma_{12}^2) < 0$.

To illustrate these complications, consider the data taken for calculating the emittance in the vertical plane for a beam energy of 55 MeV as shown in Figure 1. It is clear that the quadrupole was not scanned sufficiently far and we are relegated to fitting one-half of a parabola. However, simply fitting all 12 of the data points results in an unrealizable, complex emittance. Yet by removing three outlying data points and fitting the remaining points, a physically acceptable emittance was obtained.

At the time of this writing, the analysis of the emittance data is still in progress. However initial estimates suggest that the geometric emittance in the transverse planes with an injector energy of 55 MeV with 10 μ A of pulsed beam is on the order of $(0.5-2.5) \times 10^{-8}$ m-rad, while for an injector energy of 20 MeV the transverse emittances are roughly 2-5 times larger (see Tables 1 and 2 for normalized emittances).

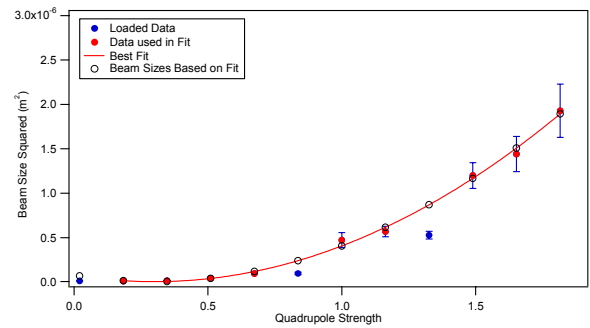


Figure 1: Vertical emittance data for $E_{inj} = 55$ MeV.

BEAM PROFILE MEASUREMENTS

Wire scanners are used throughout the CEBAF accelerator to measure the beam profile. The wire scanner mechanism drives 25 μ m tungsten wires through the electron beam, oriented in the X, XY and Y axes. The standard CEBAF wire scanner measures the induced current on the wire due to secondary emission of electrons from the wire. These induced currents tend to be in the nA range and this system is well suited to measuring the core σ of beam and have a dynamic range of about 100. To improve on the dynamic range of the wire scanner for beam profile measurements of the energy recovered beam, instrumentation was added to the wire scanner just upstream of the beam dump. This instrumentation relies on photomultiplier tubes to detect the scattered electron or the subsequent shower from the incident beam intercepting the wire [3]. The beam currents for the energy recovery experiment are large (tens of μ A) compared to those previously measured using this method in CEBAF's Hall-B (nA range) where photomultipliers are used routinely.

The beam profiles for the energy recovered beam are processed in a manner similar to that described in Reference [4]. Instead of merging data from wires of different diameters, the photomultipliers were operated with different gains. The data are combined to yield a beam profile with greater dynamic range than one would obtain using a single photomultiplier or by measuring the induced current on the wire. Fits were performed with the data. The Y (vertical) profile for both the 55 MeV and 20 MeV recovered beam are well represented by a single Gaussian over the complete dynamic range. The X (horizontal) profile for the 55 MeV beams shows a small additional contribution on the left side of the plot (see Figure 2) while the 20 MeV X profile is quite broad, but Gaussian, for this portion of the experiment.

RF MEASUREMENTS

In addition to the beam based measurements presented in the previous sections, another important class of measurements deals with the RF system's response to energy recovery [5]. These measurements are intended to test the system's response by measuring the gradient and

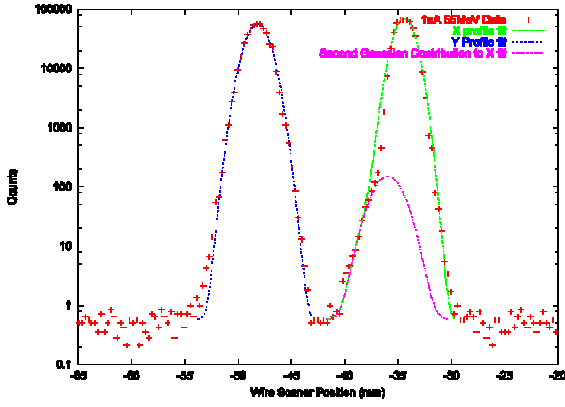


Figure 2: Large dynamic range X and Y beam profile measurement of energy recovered beam with E=55 MeV.

phase stability with and without energy recovery in several cavities throughout the north and south linac. As an example, consider Figure 3 which illustrates the RF system gradient modulator drive signal during pulsed beam operation. Without energy recovery this signal is nonzero when a 250 μ s beam pulse enters the RF cavity, indicating power is drawn from the cavity. This occurs either when the recirculation of the beam is completely impeded (as in the long pulse train) or in the period during which the head of the pulse train does not close on the machine circumference (at the leading edge of the long pulse). With energy recovery, the signal is zero once the initial transient passage of the leading edge of the pulse is over, indicating no additional power draw is required by the cavity.

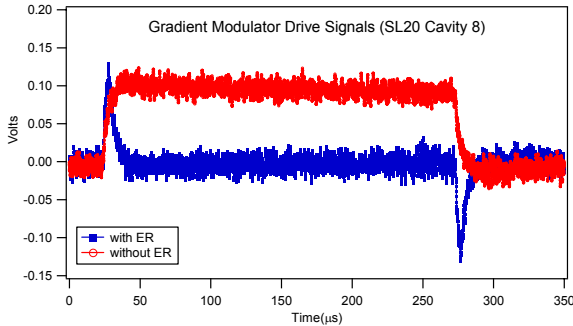


Figure 3: Gradient modulator drive signals during pulsed mode operation with and without energy recovery.

PRELIMINARY RESULTS

Although further analysis is required, several conclusions can be made based upon the available data. The first is that we were able to measure the beam profile of the energy recovered beam with up to 10^5 dynamic range with no measurable halo (i.e. particles outside a Gaussian core). The second, based upon the phase space measurements in Tables 1 and 2, is that the emittance is degraded by passage through the linacs. Possible causes are [6] cavity fundamental power coupler dipole mode driven steering and cavity higher order mode coupler

induced transverse coupling. The third and perhaps the most salient conclusion is that the energy recovery process does not contribute significantly to the emittance degradation since the degradation of the recirculating pass is consistent with that of the accelerating pass.

Location	Normalized Emittance (mm-mrad)	$\delta p/p$ (10^{-3})	E_{beam} (MeV)
Injector (1 st pass)	$\epsilon_x = 0.119798$ $\epsilon_y = 0.188577$	0.029010	55
Arc 1 (1 st pass)	$\epsilon_x = 0.434472$ $\epsilon_y = 0.256338$	0.007980	555
Arc 2 (1 st pass)	$\epsilon_x = 2.393010$ $\epsilon_y = 2.064720$	0.019811	1055
Extraction (2 nd pass)	$\epsilon_x \sim (0.538 - 1.184)$ $\epsilon_y \sim (1.184 - 2.799)$		55

Table 1: Phase space measurements for $E_{inj} = 55$ MeV.

Location	Normalized Emittance (mm-mrad)	$\delta p/p$ (10^{-3})	E_{beam} (MeV)
Injector (1 st pass)	$\epsilon_x = 0.100796$ $\epsilon_y = 0.090427$	0.036966	20
Arc 1 (1 st pass)	$\epsilon_x = 0.280880$ $\epsilon_y = 0.253402$	0.007155	520
Arc 2 (1 st pass)	$\epsilon_x = 0.674722$ $\epsilon_y = 0.451146$	0.010000	1020
Extraction (2 nd pass)	$\epsilon_x \sim (0.899 - 0.978)$ $\epsilon_y \sim (1.956 - 5.869)$		20

Table 2: Phase space measurements for $E_{inj} = 20$ MeV.

ACKNOWLEDGMENTS

We would like to thank H. Dong, A. Hofler, C. Hovater, L. Merminga, and T. Plawski for performing the required RF measurements and J. Bengston for assistance with the emittance and energy spread measurements.

REFERENCES

- [1] Bogacz, A. et al. Proceedings of this conference.
- [2] *Ibid.*
- [3] C. Tennant, "An Overview of Emittance Measurements in CEBAF-ER", TN-03-004, 2003.
- [4] A. Freyberger, "Large Dynamic Range Beam Profile Measurements" Proceedings of this conference.
- [5] Bogacz, A. et el. Proceedings of this conference.
- [6] Z. Li, "Beam Dynamics in the CEBAF Superconducting Cavities", PhD Thesis, William and Mary, 1995.